Hernandez, Javier; Romero, Victor; Escalante, Alfredo; Toriz, Guillermo; Rojas, Orlando J.; Sulbaran, Belkis

Agave tequilana Bagasse as Source of Cellulose Nanocrystals via Organosolv Treatment

Published in:
BioResources

DOI:
10.15376/biores.13.2.3603-3614

Published: 01/01/2018

Document Version
Publisher's PDF, also known as Version of record

Published under the following license:
Unspecified

Please cite the original version:
Hernandez, J., Romero, V., Escalante, A., Toriz, G., Rojas, O. J., & Sulbaran, B. (2018). Agave tequilana Bagasse as Source of Cellulose Nanocrystals via Organosolv Treatment. *BioResources*, *13*(2), 3603-3614. https://doi.org/10.15376/biores.13.2.3603-3614

Agave tequilana Bagasse as Source of Cellulose Nanocrystals *via* Organosolv Treatment

Javier Hernández,[a] Víctor Romero,[a] Alfredo Escalante,[b] Guillermo Toríz,[b] Orlando J. Rojas,[c] and Belkis Sulbarán [a,*]

Cellulose nanocrystals (CNCs) were isolated from *Agave tequilana* residues derived from ethanol production. Hemicelluloses and lignin extraction from agave bagasse was carried out *via* organosolv (ethanol/acetic) digestion followed by conventional sulfuric acid hydrolysis. The ethanol/acetic acid treatment resulted in cellulose yields of approximately 67% after lignin and ash removal. Compared to soda and sodium chlorite treatments with organosolv, the time and chemical load needed for delignification were remarkably reduced. The morphology of the cellulose fiber obtained in the three treatments was between 0.55 and 0.62 mm, with which CNC was obtained in the order of 83 to 195 nm in length. It is noteworthy that the longest cellulose fibers and nanocrystals were obtained from organosolv cellulose. The organosolv treatment led to a high purity cellulose, derived CNCs with a minimum energy consumption and mild chemical usage, and also considered the use of material streams associated with distillation processes. Thus, a viable alternative is suggested for the production of high quality CNC from widely available residual biomass that otherwise poses environmental and health-related risks.

Keywords: Agave bagasse; Isolation; Green chemistry; Cellulose nanocrystals; Tequila; Residual biomass; Bagasse

*Contact information: a: Department of Water and Energy, University of Guadalajara Campus Tonalá; b: Department of Wood, Cellulose and Paper, University of Guadalajara, University Center of Exact Sciences and Engineering (CUCEI); c: Department of Bioproducts and Biosystems, School of Chemical Engineering, Aalto University; *Corresponding author: belkis.sulbaran@academicos.udg.mx*

INTRODUCTION

There is an urgent need to pursue green technologies to address current and future challenges. Specifically, the search for new materials must consider available local resources and minimization of the environmental impact associated with their synthesis (Bilal *et al.* 2017). An exemplary case is the well-established and large Tequila industry located in the western region of Mexico, which is constantly increasing its production. Tequila is obtained from a monocotyledonous plant (*Agave tequilana* Weber *var. azul)* that produces fructose and polysaccharides that, upon hydrolysis, become the main source of fermentable sugars for ethanol production. After a growth period of 6 to 8 years, the leaves of the *Agave tequilana* are removed and the core is steamed for 24 h to 48 h to hydrolyze fructans into fermentable sugars (Idarraga *et al.* 1999; Íñiguez *et al.* 2011). The solid residue is the agave bagasse, central to this study, which is composed mainly of cellulose, hemicelluloses, and lignin (50.0 wt%, 23.0 wt%, and 21 wt%, respectively) (Idarraga *et al.* 1999; Íñiguez *et al.* 2011; Robles *et al.* 2015).

The industrialization of tequila production has led to extensive farming, causing environmental deterioration and the production of vast amounts of waste. Indeed, agave bagasse represents approximately 40% of the total dry weight of agave, and 400,000 tons are generated annually, most of which are used as compost (Consejo Regulador del Tequila 2017; Alemán-Nava *et al*. 2018)

The importance of lignocellulosic residues in new applications is increasing rapidly, and methods for processing have been considered (Arevalo-Gallegos *et al*. 2017). Several authors have extracted cellulose from monocotyledons *via* traditional alkaline methods, including soda and $NaClO_2$ bleaching (Espino *et al*. 2014; Robles *et al.* 2015). In this research, the authors focused on the extraction of cellulose by organosolv solvents to then obtain cellulose nanocrystals *via* acid hydrolysis. In the organosolv process, lignin is solubilized, resulting in high yields and almost total delignification. Research on cellulose nanocrystals is focused on a wide range of potential applications, such as optical devices, barrier membranes, reinforcements for other materials, using their colloidal characteristics, and their ability to form solid films, emulsions, foams, and gels (Morán *et al.* 2008; Espino *et al.* 2014; Robles *et al.* 2015). Some of these materials can benefit from the products of tequila processing.

The aim of this study was to understand how the extraction method influences the properties of cellulose fiber isolated from the agave bagasse and the properties of the obtained nanocrystals. The nanocrystals obtained were analyzed in their physicochemical properties to determine the possible valorization of these products in high added value nanomaterials. The results were compared with reference processes, such as soda pulping (Halim 2014) and sodium chlorite delignification. The authors' hypothesis is based on the fact that organosolv methods have considerable potential in terms of delignification selectivity and environmental impact because this process is a sulfur-free method, based on the extraction of lignin by its dissolution in organic solvents at high temperature and pressure (Robles *et al.* 2018). Following acid hydrolysis of the cellulose-rich material, the authors obtained cellulose nanocrystals (CNC) and analyzed their morphology, crystallinity, and other properties.

EXPERIMENTAL

Materials

Bagasse from *Agave tequilana* Weber *var*. *azul* was collected from tequila distillery Cava de Oro in the village of Arenal Jalisco, Mexico. Aqueous solutions of $NaClO_2$ (80%), CH_3COOH (99%), KOH (90%), NaOH (97%), and H_3BO_3 (99.5%) were used for cellulose extraction and purchased from Sigma-Aldrich (Toluca, Mexico). Sulfuric acid was also purchased from Sigma-Aldrich (Toluca, Mexico).

Agave bagasse fibers were obtained by steaming the agave stem (Jiménez *et al.* 2011). The material was already depithed with a rake. The chemical composition of agave bagasse was determined *via* the standard TAPPI methods. Extractives from acetone and water were determined using TAPPI T280 pm-99 (1999) and TAPPI T207 cm-99 (1999), respectively. Acid-insoluble lignin was determined according to TAPPI T222 om-02 (2002). Ash content was determined following TAPPI T211 om-02 (2002) and α-cellulose content was determined according to TAPPI T203 cm-99 (1999). All the experiment was carried out for triplicate, and the data shown are averages with standard deviation calculations using Statistics and Machine Learning Toolbox with MatLab.versión 2015.

Methods

Treatment for cellulose fiber extraction from agave bagasse

To optimize cellulose extraction, three different pulping methods were employed to improve the yield, chemical load, and cellulose quality and purity.

(1) Organosolv treatment: ethanol and acetic acid were used for bagasse treatment as described by Gutiérrez *et al.* (2016). The bagasse fibers were milled and sieved at particles size of 60 meshes. Then, 400 grams of dry weight fibers of bagasse were placed in a 5L high pressure digester. Two liters of distilled water was added with 2 liters of ethanol and 12 milliliters of acetic acid. The temperature and time were set at 175 °C and 2.5 h, respectively. After cooling, the fibers were washed with distilled water, and the excess liquor was extracted and saved for further experiments. Hemicelluloses were extracted with KOH (24% w/v) overnight at room temperature, filtered, washed with deionized (DI) water, and then washed three times with ethanol and subjected to bleaching for 1 h. Finally, the recovered solid matter was placed overnight at room temperature in a solution of NaOH (17.5% w/v) and H_3BO_3 (4% w/v) for cellulose purification. The sample was filtered and first washed with DI water, next with solution acetic acid and distilled water (1:4), and finally washed with distilled water to remove acid.

(2) Soda treatment: NaOH was added as a solution. Distilled water was added in a ratio of 1:10 along with 70 grams of NaOH. The temperature was set to 195 °C for 1 h. After cooling, the fibers were washed with DI water. The same procedure as described in (1) was applied for hemicellulose extraction and cellulose purification.

(3) Sodium chlorite treatment: Solutions containing $NaClO_2$ and acetic acid were used to remove lignin from the agave bagasse (Espino *et al.* 2014; Robles *et al.* 2015). The DI water was added at a 1:25 ratio in a bath heated to 75 °C. Five doses of $NaClO_2$ (80% w/v) and CH_3COOH (99% w/v) were added every 12 h. Then, the fibers were thoroughly washed with distilled water. The same procedure used in the organosolv method was applied for hemicellulose extraction and cellulose purification.

CNC isolation

The CNCs obtained from the agave bagasse after each of the three treatments were prepared as described by Morán *et al.* (2008). Hydrolysis was conducted with a solid: sulfuric acid (64%) ratio of 1:10 at 45 °C for 45 min under mixing. The reaction was stopped by the addition of cool DI water (a tenfold addition level relative to dispersion volume). Sedimentation occurred overnight and was followed by centrifugation at 8500 rpm for 15 min, dialyzed with water for four days until a neutral pH was reached and ultrasonication was carried out for 10 min.

Characterization of cellulose

Cellulose fiber morphology was assessed for the three types of cellulose obtained from the agave bagasse using a fiber quality analyzer (FQA) (OpTest Equipment Inc., Hawkesbury, Ontario, Canada) and scanning electron microscope (SEM) (TESCAN, Brno-Kohoutovice, Czech Republic). The fiber length, curl index, kink index, fiber width, and coarseness were obtained. The FQA was calibrated according to TAPPI T271 om-07 (2007). For electron microscopy, the fiber samples were mounted on brass studs and, after gold coating (Laurell Technologies Corporation, North Wales, PA, USA), were imaged with a scanning electron microscope (model MIRA 3 LMU; TESCAN, Brno-Kohoutovice, Czech Republic). The cellulose yield percentages of the three treatment methods were

calculated with Eq. 1, where M_R (g) is the recovered sample, M_S (g) is the bagasse sample, and C (%) is cellulose content (44.5%):

$$Yield\ (\%) = \frac{M_R}{M_S * C} * 100 \quad (1)$$

The ash content (wt%) was determined following TAPPI T211 om-02 (2002). The degree of polymerization in the cellulose samples was determined according to the intrinsic viscosity of cellulose as described in ASTM D1795-62 (1962). Fourier transform infrared (FT-IR) spectra were obtained with a Spectrum GX spectrometer (PerkinElmer, Waltham, MA, USA) carried out in the 4000 cm^{-1} to 550 cm^{-1} range with a resolution of 4 cm^{-1}. Thermogravimetric analysis (TGA) was performed with a TGA/DSC1 STAR e. System (Mettler Toledo, Mexico City, Mexico) instrument. Temperature programs for dynamic tests were run from 25 °C to 700 °C at a heating rate of 10 °C/min. These tests were conducted under an air atmosphere (20 mL/min).

CNC characterization

The CNCs obtained from the agave bagasse after each of the three treatments used were characterized for crystallinity degree with a powder X-Ray diffractometer (XRD; D500 Model Kristallograph (Siemens, Washington D.C., USA) with a Cu Ka radiation (0.1542 nm wavelength). High angle XRD data were collected from 5° to 50° at 0.02° increments and 1 min count times using films placed on a quartz sample holder. Measurements were performed for cellulose and CNC. The relative crystallinity (%) was calculated with Eq. 2 as described by Segal *et al.* (1959),

$$IC = \left[\frac{(I_{002} - I_{am})}{I_{002}}\right] x\ 100 \quad (2)$$

where IC (%) is crystallinity degree , I_{002} is the crystalline peak of the maximum intensity at 2θ between 22° and 23° for cellulose I, and I_{am} is the crystalline peak of the minimum intensity at 2θ between 18° and 19° for cellulose I (Sulbarán *et al.* 2014).

A Digital Instruments NanoScope III controller with a MultiMode Atomic Force Microscopy (AFM) (Bruker, Billerica, USA) head was used to image the CNCs. Samples were prepared *via* spin-coating of a CNC suspension at 0.01 wt% on a mica substrate and dried at room temperature. Images were acquired in contact mode and analyzed using ImageJ 1.45 software (National Institutes of Health, Bethesda, MD, USA) to estimate the aspect radio.

RESULTS AND DISCUSSION

The chemical composition of the agave bagasse was consistent with existing literature (Íñiguez *et al.* 2011; Kestur *et al.* 2013; Robles *et al.* 2015). Cellulose is the main component in bagasse (44.5 ±2.5%). The high content of cellulose makes it a suitable raw material for CNC extraction. In bagasse hemicelluloses are lower in content (25.3 ±3.4%) due to the sugar degradation that occurs during the tequila production, where the extracting a considerable part of the sugars for the further alcohol production.

Figure 1 includes the scanning electron micrographs of the fibers before (Fig. 1A) and after (Fig. 1B, 1C, and 1D) treatment. Similar to other plant fibers, Fig. 1A shows the arrangements of fibrils and pith along the fiber axis (Espino *et al.* 2014). In the case of bagasse, a small microfibrillar angle was observed, and given the compact or tight

structure, aggressive hydrolysis was employed to break down the cell wall, which is also the case of other fibers with low helical angles, such as sisal (Siqueira *et al.* 2009; Robles *et al*. 2015). The presence of particles (likely inorganic) was observed (Fig. 1) after treatment with sodium chlorite. This finding contrasted with Fig. 1C and Fig. 1D, which display smooth fiber surfaces after treatment with the organosolv and soda methods.

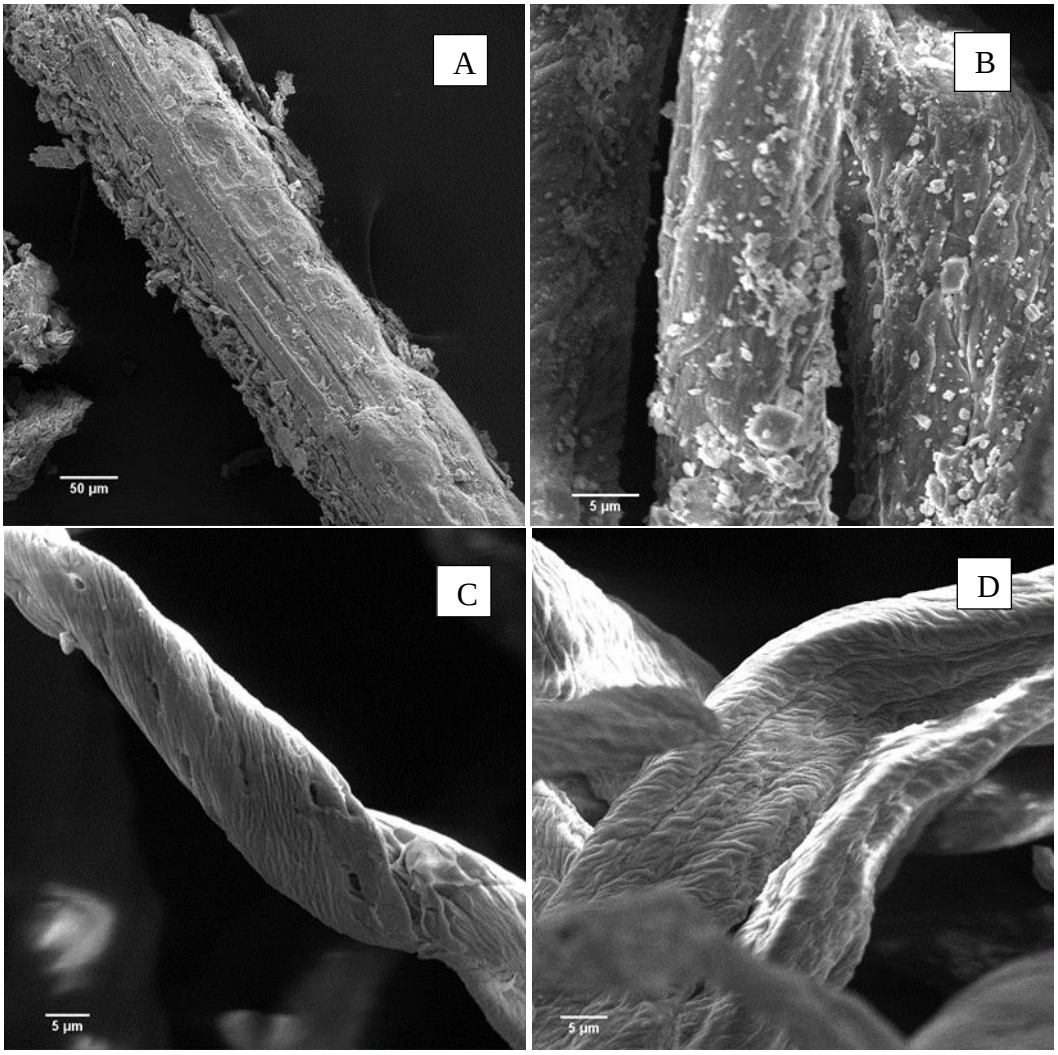

Fig. 1. SEM images of A) fibers of agave bagasse and fibers after (B) sodium chlorite, C) organosolv, and D) soda treatments µm

Table 1. Fiber Morphology after FQA Analysis

Treatment	Length Weighted (mm)	Weight Weighted (mm)	Mean Curl (Length Weighted)	Kink Angle (°)
Organosolv	0.62 ±0.009	1.3 ±0.009	0.115 ±0.009	23.8
Chlorite	0.55 ±0.010	1.41 ±0.010	0.105 ±0.010	24.3
Soda	0.57 ±0.008	1.32 ±0.008	0.087 ±0.008	19.7

The length (FQA) of the cellulose fibers was 0.5 mm to 0.6 mm before treatment (Table 1). After disassembly of the lignocellulosic matrix, cellulose macrofibrils were more accessible for the cellulose nanocrystal extraction process due to the removal of non-cellulosic components and the increased surface area (Nascimento *et al.* 2016).

The cellulose yields were 69%, 56%, and 67% after chlorite, soda, and organosolv treatment, respectively (Table 2). The crystallinity degree of the cellulose samples after treatment was between 63% and 68%. The organosolv cellulose the crystallinity degree was 68%, slightly low compared to that reported by Kestur *et al.* (2013), which was 70%. However, the crystallinity degree depends on the type of chemical treatment performed on the material and the conditions applied. The degree of crystallinity is important in the isolated cellulose nanocrystal, because acid hydrolysis dissolve non-crystalline regions of the cellulose structures (Robles *et al*. 2018).

The degree of polymerization (DP) is another important parameter for obtaining cellulose nanocrystals. In this investigation we found DP in the range from 460 to 625. The DP of a cellulose sample was rapidly reduced to a relatively constant value upon being subjected to severe conditions hydrolyzing treatments, as in the case of the chlorite treatment, and the observed DP was 460. The initial rapid DP degradation phase corresponds to the hydrolysis of the reactive amorphous region of cellulose; while the slower plateau rate phase corresponds to the hydrolysis of the slowly reacting crystalline fraction of cellulose (Hallac and Ragauskas 2011). In the case of organosolv cellulose, the DP was 500, which indicates that the pretreatment was less aggressive than pretreatment with sodium chlorite.

Table 2. Main Characteristics of Cellulose after Treatment of Agave Bagasse

Method Cellulose Extraction	Yield (%)	Ash Content (%)	Degree of Polymerization	Crystallinity degree (%)
Organosolv	67 ±3.2	1.1 ±0.10	500 ±15.28	66 ±2.24
Sodium chlorite	69 ±2.4	7.9 ±0.29	460 ±17.99	63 ±2.27
Soda	56 ±2.7	0.7 ±0.13	625 ±26.30	68 ±1.05

The FTIR spectra (Fig. 2) showed the peaks associated with lignocellulosic material.

Signals between 3600 cm^{-1} and 3000 cm^{-1} correspond to OH vibration. The band between 3000 cm^{-1} and 2600 cm^{-1} corresponds to asymmetric and symmetric C-H stretching vibrations. Moreover, the peaks at approximately 1430 cm^{-1}, 1162 cm^{-1}, and 1111 cm^{-1} represent CH2 symmetric bending, asymmetric C-O-C bridge stretching, and anhydroglucose ring asymmetric stretching, respectively. They are associated with the crystalline part of the cellulose, and the peak at approximately 893 cm^{-1} is assigned to C-H deformation of cellulose associated to the non-crystalline cellulose. In the sample without treatment, the peak of 1600 cm^{-1} corresponding to the aromatic ring (C=C) of lignin is observed.

In the following treatments, soda, chlorite and organosolv peaks decreased and corresponded to lignin residual (Schwanninger *et al.* 2004; Morán *et al.* 2008; Íñiguez *et al.* 2011).

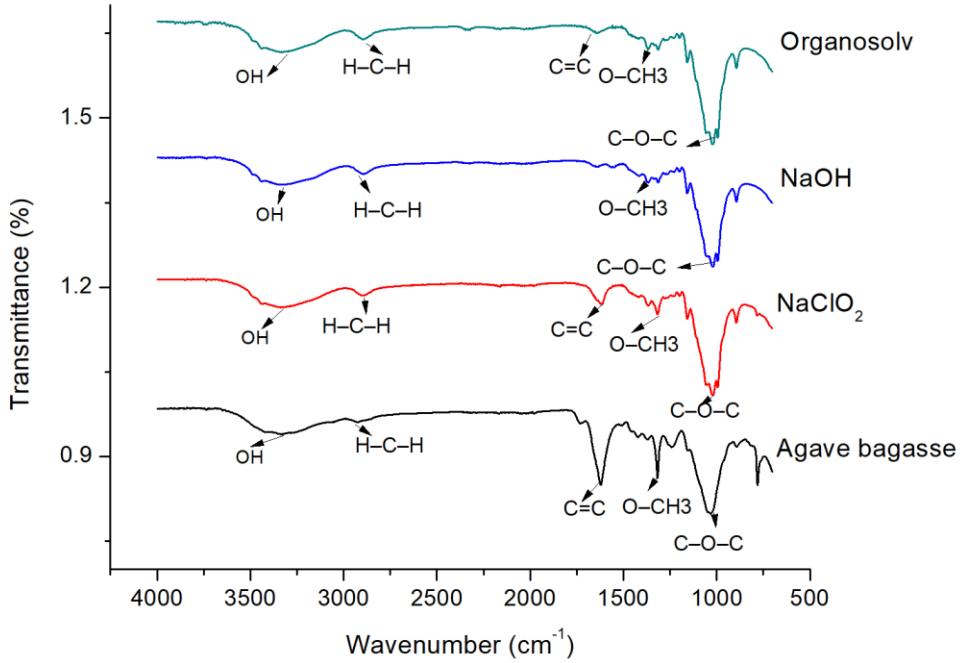

Fig. 2. FTIR spectra for agave bagasse and celluloses obtained after treatment with organosolv, soda (NaOH), or chlorite ($NaClO_2$)

The thermal gravimetric analyses indicated the decomposition of the obtained celluloses after the given treatments (organosolv, soda, and chlorite). Figure 3 shows the loss of mass (wt%) as a function of temperature.

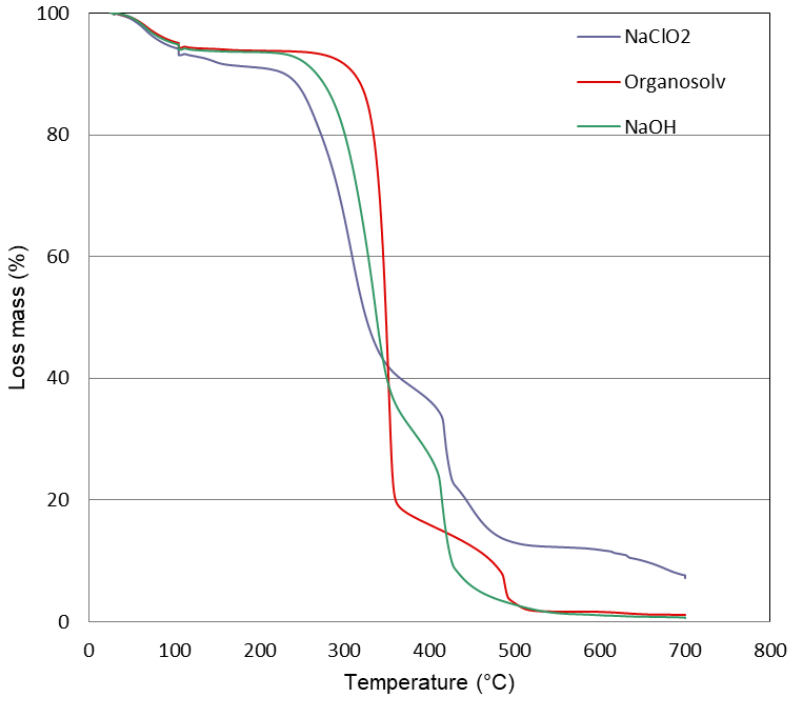

Fig. 3. Thermal analysis of celluloses obtained for the different methods

Three weight loss events can be identified, which are the evaporation of water adsorbed on the cellulose, cellulose degradation, and the oxidation and breakdown of charred residues. The water evaporation occurred between 30 °C and 140 °C with a mass loss of < 6%. During the degradation of the cellulose, different processes occur, including depolymerisation, dehydration, and decomposition of glyosidic units (Espino *et al.* 2014). The samples obtained after sodium chlorite treatment had a more pronounced weight loss (10 wt%) up to 230 °C, followed by a loss of 60% between 230 ºC and 340 ºC to finally reach a solid residues content (mainly ash) of approximately 6 wt%. Soda treatment also had a similar behavior, yet the ash content was nearly zero. Samples after the organosolv treatment showed an onset of thermal degradation at 260 ºC, a step weight loss of more than 80% between 260 °C to 360 °C, and negligible residues. The observations indicated a homogeneous material amenable to hydrolysis with good yields.

Cellulose nanocrystals

Figure 4 includes AFM images (1 µm × 1 µm and 3 µm × 3 µm) for all CNC samples, which exhibited typical rod-like morphology with a length of approximately 100 nm to 250 nm and a width of approximately 15 nm to 45 nm. Statistical analyses of nanocrystal dimensions from AFM images were performed using ImageJ software. Geometric dimension data for all CNC samples are summarized in Table 3.

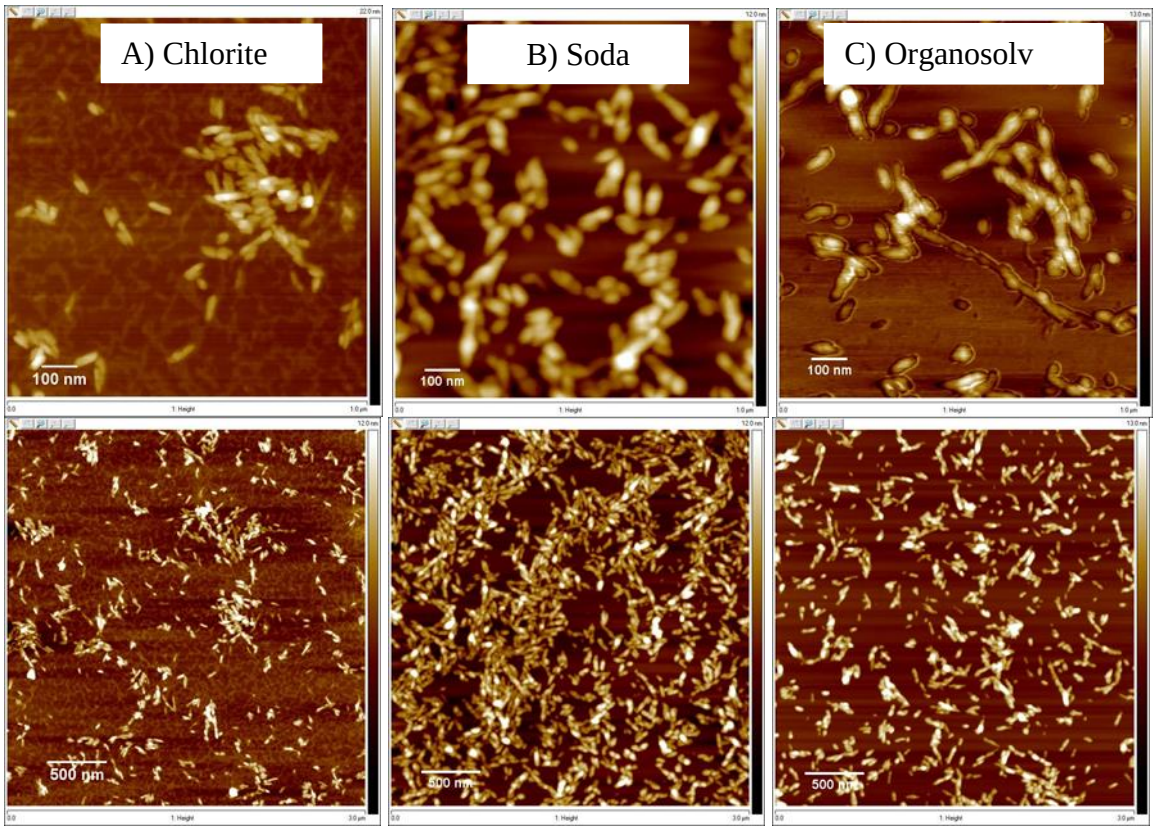

Fig. 4. AFM images (3 µm × 3 µm) of CNCs isolated from cellulose after treatment with the A) Chlorite, B) soda, and C) organosolv

Table 3. Dimensions, Aspect Ratio, and Zeta Potential of CNC Samples

CNC	Length (nm)	Diameter (nm)	L:D	Zeta Potential (mV)
Sodium chlorite	83 ±24.0	25 ±6.0	3.4	-25 ±1.70
Soda	133 ±28.1	41 ±9.9	3.2	-38 ±4.18
Organosolv	195 ±37.2	42 ±7.8	4.6	-44 ±2.82

The CNCs obtained after chlorite treatment showed the smallest length and width, and they were the largest for the organosolv CNC. Furthermore, for the three samples, the dimensions of the CNCs from cellulose bagasse indicated a relatively low aspect ratio (L:D). The L:D ratio is one of the key parameters for CNC utilization as nanofillers in nanocomposites (Espino *et al.* 2014). The dimension changes were attributed to the elimination of the non-crystalline component, as the cellulose crystallinity was lower for the CNC obtained after chlorite treatment.

The negative zeta potential originated from the half sulfate esters group ($-OSO_3^-$) on CNC introduced after sulfuric acid hydrolysis *via* esterification (sulfation) between surface hydroxyls and H_2SO_4 (Lin and Dufresne 2014b). The hydrolyzed CNCs were highly negatively charged and formed a well-dispersed aqueous colloidal suspension. The surface charge is affected by the severity of acid hydrolysis (Lin and Dufresne 2014a).

With the results obtained in all the characterization, it is important to say that cellulose was extracted from waste generated during tequila production with organosolv processes. These process are sulfur-free, and this makes it have a low environmental impact. Analyzed properties were within the expected criteria (dimensions, colloidal stability, and crystallinity) and represent a suitable valorization for rather undervalued side-streams. When comparing the organosolv CNC with cellulose from other non-wood plants, they are notably smaller (Robles *et al.* 2018). However, these characteristics depend on their final application as can be biomedicine, pharmacy and materials science.

CONCLUSIONS

1. When comparing the three procedures, important differences were noticed in terms of yield, fiber quality, and size distribution, among others. Organosolv is an environmentally friendly treatment because it is chlorine-free and fewer delignification cycles were used compared to the other methods, thus reducing the energy and chemicals used.
2. Compared to the chlorite treatment, the soda and organosolv methods delivered fairly good yields of cellulose after digestion, using short times and less chemical load. The ash content was relatively high after chlorite treatment, but it was reduced by half *via* acid treatment. However, in the case of soda and organosolv pretreatments, the ash content was below 1%, making the acid treatment unnecessary. The SEM images provided clear evidence that these pretreatments resulted in cleaner surfaces.
3. Organosolv cellulose of bagasse blue agave are a good source to produce value-added products as cellulose nanocrystals. The nanoscale dimensions and the distribution of CNC were demonstrated. Nanocrystal cellulose diameter sizes were 45 ±7.8 nm, and the length size was 195 ±37.2 nm.

ACKNOWLEDGMENTS

Financial support for this work was provided by the National Council of Science and Technology of Mexico (CONACYT). The authors thank Aalto University in Finland for experimental support during the CNC extraction.

REFERENCES CITED

Alemán-Nava, G., Gatti, I., Parra-Saldivar, R., Dallemand, J.-F., Rittmann, B. E., and Iqbal, H. M. N. (2018). "Biotechnological revalorization of Tequila waste and by-product streams for cleaner production – A review from bio-refinery perspective," *Journal of Cleaner Production* 172, 3713-3720. DOI: 10.1016/j.jclepro.2017.07.134

ASTM D1795-62 (1962). "The standard test method for intrinsic viscosity of cellulose," ASTM International, West Conshohocken, PA.

Arevalo-Gallegos, A., Ahmad, Z., Asgher, M., Parra-Saldivar, R., and Iqbal, H. M. N. (2017). "Lignocellulose: A sustainable material to produce value-added products with a zero waste approach—A review," *International Journal of Biological Macromolecules* 99, 308-318. DOI:10.1016/j.ijbiomac.2017.02.097

Bilal, M., Asgher, M., Iqbal, H. M. N., Hu, H., and Zhang, X. (2017). "Biotransformation of lignocellulosic materials into value-added products—A review." *International Journal of Biological Macromolecules* 98, 447-458. DOI:10.1016/j.ijbiomac.2017.01.133

Consejo Regulador del Tequila [Tequila Regulatory Council] (2017). "Estadistica producción total: Tequila y tequila 100% [Total production statistics: Tequila and 100% tequila]," (https://www.crt.org.mx/EstadisticasCRTweb/), Accessed 11 Dec 2017.

Espino, E., Cakir, M., Domenek, S., Román-Gutiérrez, A. D., Belgacem, N., and Bras, J. (2014). "Isolation and characterization of cellulose nanocrystals from industrial by-products of *Agave tequilana* and barley," *Industrial Crops and Products* 62, 552-559. DOI: 10.1016/j.indcrop.2014.09.017

Gutiérrez-Hernández, J. M., Escalante, A., Murillo-Vázquez, R. N., Delgado, E., González, F. J., and Toríz, G. (2016). "Use of Agave tequilana-lignin and zinc oxide nanoparticles for skin photoprotection," *Journal of Photochemistry and Photobiology B: Biology* 163, 156-161. DOI:10.1016/j.jphotobiol.2016.08.027

Halim, A. E. S. (2014). "Chemical modification of cellulose extracted from sugarcane bagasse: Preparation of hydroxyethyl cellulose," *Arabian Journal of Chemistry* 7(3), 362-371. DOI: 10.1016/j.arabjc.2013.05.006

Hallac, B. B., and Ragauskas, A. J. (2011). "Analyzing cellulose degree of polymerization and its relevancy to cellulosic ethanol," *Biofuels, Bioprod. Bioref* 5, 215-225. DOI:10.1002/bbb.269

Íñiguez, G., Valadez, A., Manríquez, R., and Moreno, M. V. (2011). "Utilization of by-products from the tequila industry. Part 10: Characterization of different decomposition stages of *Agave Tequilana* webber bagasse using FTIR spectroscopy, thermogravimetric analysis and scanning electron microscopy," *Revista Internacional de Contaminación Ambiental* 27(1), 61-74.

Jiménez, J. E., Urista, C. M., and Estupiñán, J. C. (2011). "Optimización del proceso de ultrafiltración de efluentes de una industria de cereales [Optimization of the

ultrafiltration process of effluents from a cereal industry]," *Afinidad* 68(552), 116-123.

Kestur, S. G., Flores-Sahagun, T. H. S., Dos Santos, L. P., Dos Santos, J., Mazzaro, I., and Mikowski, A. (2013). "Characterization of blue agave bagasse fibers of Mexico," *Composites Part A: Applied Science and Manufacturing* 45, 153-161. DOI: 10.1016/j.compositesa.2012.09.001

Lin, N., and Dufresne, A. (2014a). "Nanocellulose in biomedicine: Current status and future prospect," *European Polymer Journal* 59, 302-325. DOI: 10.1016/j.eurpolymj.2014.07.025

Lin, N., and Dufresne, A. (2014b). "Surface chemistry, morphological analysis and properties of cellulose nanocrystals with gradiented sulfation degrees," *Nanoscale* 6(10), 5384-5393. DOI: 10.1039/c3nr06761k

Morán, J. I., Alvarez, V. A., Cyras, V. P., and Vázquez, A. (2008). "Extraction of cellulose and preparation of nanocellulose from sisal fibers," *Cellulose* 15(1), 149-159. DOI: 10.1007/s10570-007-9145-9

Nascimento, D. M. d., Almeida, J. S., Vale, M. d. S., Leitão, R. C., Muniz, C. R., Figueirêdo, M. C. B. d., Morais, J. P. S., and Rosa, M. d. F. (2016). "A comprehensive approach for obtaining cellulose nanocrystal from coconut fiber. Part I: Proposition of technological pathways," *Industrial Crops and Products* 93, 66-75. DOI: 10.1016/j.indcrop.2015.12.078

Robles, E., Fernández-Rodríguez, J., Barbosa, A. M., Gordobil, O., Carreño, N. L.V., and Labidi, J. (2018). "Production of cellulose nanoparticles from blue agave waste treated with environmentally friendly processes," *Carbohydrate Polymers* 183, 294-302. DOI: 10.1016/j.carbpol.2018.01.015

Robles, E., Urruzola, I., Labidi, J., and Serrano, L. (2015). "Surface-modified nano-cellulose as reinforcement in poly(lactic acid) to conform new composites," *Industrial Crops and Products* 71, 44-53. DOI: 10.1016/j.indcrop.2015.03.075

Schwanninger, M., Rodrigues, J. C., Pereira, H., and Hinterstoisser, B. (2004). "Effects of short-time vibratory ball milling on the shape of FT-IR spectra of wood and cellulose," *Vibrational Spectroscopy* 36(1), 23-40. DOI: 10.1016/j.vibspec.2004.02.003

Segal, L., Creely, J., Martin, A., and Conrad, C. (1959). "An empirical method for estimating the degree of crystallinity of native cellulose using the X-ray diffractometer," *Textile Research Journal* 29(10), 786-794.

Siqueira, G., Bras, J., and Dufresne, A. (2009). "Cellulose whiskers *versus* microfibrils: Influence of the nature of the nanoparticle and its surface functionalization on the thermal and mechanical properties of nanocomposites," *Biomacromolecules* 10(2), 425-432. DOI: 10.1021/bm801193d

Sulbarán, B., Toriz, G., Allan, G. G., Pollack, G. H., and Delgado, E. (2014). "The dynamic development of exclusion zones on cellulosic surfaces," *Cellulose* 21(3), 1143-1148. DOI: 10.1007/s10570-014-0165-y

TAPPI T203 cm-99 (1999). "Alpha-, beta- and gamma-cellulose in pulp," TAPPI Press, Atlanta, GA.

TAPPI T207 cm-99 (1999). "Water solubility of wood and pulp," TAPPI Press, Atlanta, GA.

TAPPI T211 om-02 (2002) "Ash in wood, pulp, paper and paperboard: combustion at 525°C," TAPPI Press, Atlanta, GA.

TAPPI T222 om-02 (2002). "Acid-insoluble lignin in wood and pulp," TAPPI Press, Atlanta, GA.
TAPPI T271 om-07 (2007). "Fiber Length of pulp and paper by automated optical analyzer using polarized light," TAPPI Press, Atlanta, GA.
TAPPI T280 pm-99 (1999). "Acetone extract ives of wood and pulp," TAPPI Press, Atlanta, GA.

Article submitted: January 29, 2018; Peer review completed: March 11, 2018; Revised version received and accepted: March 24, 2018; Published: March 27, 2018.
DOI: 10.15376/biores.13.2.3603-3614